UJEAS

UNIZIK JOURNAL OF ENGINEERING AND APPLIED SCIENCES

UNIZIK Journal of Engineering and Applied Sciences 3(5), December (2024), 1382 - 1401
Journal homepage: https://journals.unizik.edu.ng/index.php/ujeas
PRINT ISSN: 2992-4383 || ONLINE ISSN: 2992-4391

# Voltage Stability Assessment of Nigeria 330 kV Power Grid: A Critical Bus Perspective

Ikenna A. Onyegbadue[1*], Stephen N. Ukagu[2] and Dennis O. Okonkwo[3]
[1,2,3] Electrical and Computer Engineering Department, College of Engineering, Igbinedion University, Okada, Edo State.
[*]Corresponding Author's E-mail: onyegbadue.ikenna@iuokada.edu.ng

**Abstract**

Voltage stability issues within Nigeria's 330 kV power grid pose significant risks to the reliability and efficiency of the power supply, hence, there is the need for urgent investigation. This research aims to assess the voltage stability of Nigeria's 330 kV Power grid with specific objectives viz; identifying critical buses and branches, assessing the effect of shunt faults on voltage stability and implementing reactive power compensation to stabilize bus voltages. A fast decoupled load flow technique was utilized to analyze the 330 kV Nigerian power system and obtain system losses alongside locating critical buses. With the aid of ETAP 12.0 software the network was modelled and shunt faults were introduced for transient studies. This provided a base to evaluate voltage stability. VAr sources were integrated to determine their effects on bus voltages and transient stability. The findings indicated that the Jebba Hydro, Shiroro Hydro, and Olorunsogo gas buses were overloaded, while the Yola and Maiduguri buses faced Undervoltage issues. The transient stability analysis demonstrated that VAr compensation effectively restored voltage stability at the critical buses. This research offers proactive strategies to ensure voltage stability in Nigeria's 330 kV power grid, thereby enhancing the reliability and efficiency of power supply

**Keywords:** voltage stability, power grid, critical buses, reactive power compensation, transient stability analysis.

## 1. Introduction

Over the past decades, the evolution of power systems has been characterized by the dominance of centralized large-scale generating stations (Hossain et al., 2019; Ismael et al., 2019). These stations transmit electrical energy over extensive distances via interconnected transmission systems, forming the backbone of modern power infrastructure (Blaabjerg et al., 2017; Mehigan et al., 2018; Ranjan Pradhan et al., 2013). The propensity for voltage instability in power systems underscores the critical importance of voltage stability assessment and monitoring for maintaining reliable operation and informed planning decisions (Danish et al., 2019; Nageswa Rao et al., 2021). Voltage instability incidents have played a key role in causing major blackouts experienced in the world. (Sharma et al., 2021). To minimize the risk of voltage collapse, it is important to include stability analysis in both the planning stages and the real-time operations of power systems (Yekini et al., 2024b; Zhu et al., 2016). Over the past years, a range of methods and mechanisms has been introduced for analyzing voltage stability (Danish et al., 2019; Zhu et al., 2016). The use of GPS-synchronized phasor measurement units for online monitoring has increased, which helps assess power system stability in real-time (Pardo-Zamora et al., 2021).

Voltage stability analysis in power systems presents a multifaceted challenge, necessitating the concurrent consideration of numerous technical complexities and interconnected factors (Madueme & Onyegbadue, 2018; Massaoudi et al., 2023; Okampo et al., 2022; Shair et al., 2021). Some of the challenges include determining network equivalent parameters for calculating stability indices and distinguishing system variations from noise in phasor measurement unit (PMU) measurements (Aminifar et al., 2021; Bu et al., 2023). The presence of noise in Phasor Measurement Unit (PMU) measurements can compromise the accuracy of voltage stability indices, leading to erroneous predictions hence, posing a substantial challenge to reliable power system monitoring and control (Biswal

et al., 2023; Danish et al., 2019; S. Das & Panigrahi, 2022). Additionally, the impact of various load models on the stability of voltage is a widely acknowledged factor (Yekini et al., 2024a). However, only a few research papers incorporate load models into the voltage stability index (VSI) formulation (Muthulakshmi et al., 2017). The effectiveness of voltage stability indices, including the Linearized Motor Voltage Stability Index (LMVSI) and the Voltage-Stability Load Bus Index (VSBLI), is compromised by inherent limitations (Rodriguez-Garcia et al., 2019). LMVSI requires precise motor parameter knowledge to capture dynamic load dynamics, whereas VSBLI's dependence on Thevenin equivalent estimation introduces vulnerability to estimation inaccuracies or data quality issues (Jiang & Meng, 2023; Ramirez & Dobson, 2014; Ramírez-P et al., 2018). Efforts have been made to improve existing indices, such as enhancing the L index to determine the saddle-node bifurcation point for different load models (L. Neves & Alberto, 2021; L. S. Neves & Costa Alberto, 2020).

However, some methods, including the original L-index formulation, may present limitations in online monitoring schemes, such as discontinuities when reactive power limits are reached during generator commutation to PQ buses (Tang et al., 2024). Sensitivity-based indices, like the sensitivity-based Thevenin index (STI), offer the potential for monitoring voltage stability from wide area measurement systems (WAMS) or state estimator data (Chintakindi et al., 2022). While STI validation has been verified on larger systems using constant power load models, future works may consider the inclusion of ZIP and exponential-type load models for further validation. Voltage collapse issues in power systems can be attributed to the system's inability to supply reactive power or excessive absorption of reactive power (Bogodorova et al., 2016; Ismail et al., 2020; Lee & Song, 2019). Comprehensive voltage stability analysis is crucial for ensuring power system resilience (Hosseinzadeh et al., 2021; Liang et al., 2022; Moheb et al., 2022; Penha da Silva Júnior et al., 2021). Various analytical techniques have been developed, including PV/QV curves, continuation power flow, multiple power flow solutions, modal analysis, and optimization-based methods (Adegoke & Sun, 2023; Gadal et al., 2023; Liu et al., 2023; Malik et al., 2024; Modarresi et al., 2016; Trias, 2018; Valuva et al., 2023). These approaches enable operators of power systems to assess and mitigate voltage instability risks (Adebayo & Sun, 2017; Mokred & Wang, 2024; Valuva et al., 2023).

The developed Three-Phase Unbalanced Continuation Power Flow algorithm was shown to be robust and effective in assessing voltage stability for various system configurations (Montoya et al., 2021; Nirbhavane et al., 2021). However, the focus was primarily on distribution systems, with the potential for extension to transmission systems.
The importance of precise forecasting methods has been emphasized by the examination of voltage instability in power systems networks using modal analysis techniques (Abdalla Seedahmed et al., 2019). This demonstrates effectiveness in assessing voltage stability and identifying critical system components. The focus was primarily on steady-state analysis; hence, transient conditions were not considered.

A review of Machine Learning approaches for online voltage stability assessment in power systems has been provided which highlights their potential to enhance power system stability and reduce blackout risks (Alimi et al., 2020; Amroune, 2021; Ozcanli et al., 2020). Discussions on the effect of transient conditions on the stability of the network were ignored. No emphasis was given to voltage instability in a practical 330 kV network.
A robust framework has been developed for the online detection of long-term voltage instability using support vector machines (Nguyen Duc et al., 2017; Villa-Acevedo et al., 2022). This framework reliably predicts voltage collapse and detects critical conditions. However, it was tested on a standard IEEE bus system, without adequate consideration for practical network systems experiencing transient conditions.

Voltage stability assessment in real time was done using Thevenin equivalent impedance estimation (Lee & Han, 2019; Polster & Renner, 2017). This algorithm effectively detected voltage stability/instability under severe contingency scenarios. The integration with phasor measurement unit technology and load model parameter estimation enhances accuracy. However, the focus was primarily on a less complex network like the Korean power system
A Load Dynamic Stability Index (LDSI) has been developed to assess short-term voltage stability more accurately by capturing load dynamics (Kasar et al., 2024; Zhang et al., 2023). The integration with the support vector machine method has enhanced accuracy. LDSI effectively captures load dynamics for short-term voltage stability assessment and enables accurate load modelling through ambient signal-based identification. The support vector machine method further improves the properties of the index, enhancing power system stability analysis. However, broader applicability to other load models and power systems has not been explored.

The growing prevalence of distributed energy resources and power electronic devices in AC distribution networks has raised concerns regarding stability and reliability (Abdukhakimov et al., 2019; Muhtadi et al., 2021). A comprehensive

review of Small-Signal Stability Analysis (SSSA) methods for AC distribution grids highlights the importance of impedance-based stability analysis in the frequency domain using the Synchronous Reference Frame (SRF) (Rahman et al., 2019). It was found that by dividing the system into load and source, accurate stability assessment could be achieved through perturbation-based impedance determination and application of the Nyquist stability criterion. This review is specifically focused on small-signal stability analysis using impedance-based SRF models and does not cover transient stability or practical 33 kV network assessments.

Nigeria's power grid has consistently faced a range of challenges, including frequent blackouts, inadequate infrastructure, and issues with voltage stability (Jimoh & Raji, 2023). These problems significantly impact the reliability and efficiency of the nation's power supply. A research study provided an overview of the challenges confronting Nigeria's power sector, specifically focusing on infrastructural inadequacies and the effects of voltage instability on power supply reliability (Dada, 2014). An investigation into the causes of power interruptions in Nigeria has been conducted, emphasizing infrastructural challenges such as insufficient transmission and distribution networks (Monyei et al., 2018). Additionally, research has been carried out on voltage stability issues within Nigeria's power grid, highlighting the risks to the reliability and efficiency of power supply (Adoghe et al., 2023). The state of infrastructure within Nigeria's power sector has been evaluated, identifying shortcomings in transmission and distribution networks that exacerbate power grid issues (Oleka et al., 2016). A study on the effects of voltage instability on power quality in Nigeria has been conducted. This research explores how voltage instability influences power quality, emphasizing the urgent need for action to address this issue (Hamoud, 2023).

The efficacy of existing voltage stability analysis methods is tempered by significant limitations. Specifically, these approaches often neglect the critical consideration of shunt fault impacts on vulnerable buses within complex networks, including the Nigeria 330 kV power system network, especially in transient conditions. As part of this research, the aim is to study the voltage stability of the Nigeria 330 kV power system network, with specific objectives including identifying critical buses and branches from loadflow studies, introducing shunt faults to study their effect on voltage stability from transient analysis in ETAP 12.0, and stabilizing voltage at the buses using VAr sources with the aid of ETAP 12.0 Software.

## 2.0 Material and Methods

ETAP 12.0 was selected for this study due to its comprehensive features, flexibility, and relevance to the Nigerian power grid. It offers a wide range of power system analysis capabilities, including load flow, short circuit, and transient stability analysis, making it an ideal choice for studying the Nigerian power grid (S. R. Das et al., 2021). Additionally, ETAP 12.0 provides flexibility and customization options, a user-friendly interface, and compatibility with Nigerian power grid data, setting it apart from other power system analysis software such as PSS/E, DigSILENT, and MATLAB (Hay & Ferguson, 2015).

This work commenced with a comprehensive analysis of the 330 kV Nigerian power system network to identify critical and marginal buses. Utilizing fast decoupled load flow methodology, the study leveraged data from the annual technical report, encompassing generator and load bus parameters and positive and zero sequence impedance data for transmission lines. The 330 kV Nigerian power system was subsequently modelled employing Electrical Transient Analyzer Program (ETAP) 12.0 software. Shunt faults (sub-transient cycle) were intentionally introduced at critical and marginal buses to investigate voltage stability, and the resultant voltage fluctuations were observed. A transient stability assessment was conducted using the adaptive Newton-Raphson technique, simulating a Line-to-Ground fault at 0.5 seconds, cleared at 10 seconds. Furthermore, Reactive Power sources (VAr sources) were integrated into the network, and their impact on bus voltages was examined.

### 2.1 Mathematical Formulations

The relationship between the bus admittance, phase voltage, and current is given by the matrix equation thus (Bazrafshan & Gatsis, 2018);

$$\begin{bmatrix} Y_{11} & Y_{12} & Y_{13} & \dots & Y_{1N} \\ Y_{21} & Y_{22} & Y_{23} & \dots & Y_{2N} \\ Y_{31} & Y_{32} & Y_{33} & \dots & Y_{3N} \\ . & . & . & & . \\ . & . & . & & . \\ . & . & . & & . \\ Y_{N1} & Y_{N2} & Y_{N3} & \dots & Y_{NN} \end{bmatrix} \begin{bmatrix} V_1 \\ V_2 \\ V_3 \\ . \\ . \\ . \\ V_N \end{bmatrix} = \begin{bmatrix} I_1 \\ I_2 \\ I_3 \\ . \\ . \\ . \\ I_N \end{bmatrix} \quad (1)$$

$$YV = I \quad (2)$$

The Y matrix represents the admittance of an N-by-N electrical system. V is the column of voltages for N-buses, and I is the column of currents for those buses.

$$Y_{ii} = \sum_{k \in i} y_{ik} \quad (3)$$

Where $y_{ik}$ is the admittance between buses i and k and $k \in i$ denotes that the k bus is connected to bus i.
The line current $I$ as a function of the electric load complex apparent power is given thus;

$$S = P_L + jQ_L \quad (4)$$

$$I = \frac{S}{V_r} = \frac{P_L - jQ_L}{V_r} \quad (5)$$

S : Complex power (kVA) demanded by the load on the distribution system
$P_L$ : Real power demanded by the load
$Q_L$ : Reactive power demanded by the load (usually an inductive load)
$V_r$ : Voltage at the load bus (receiving end).
$V_s$ : Voltage at the sending end of the network.
Consider the phasor diagram of the voltage in a typical power system network as shown in Figure 1.

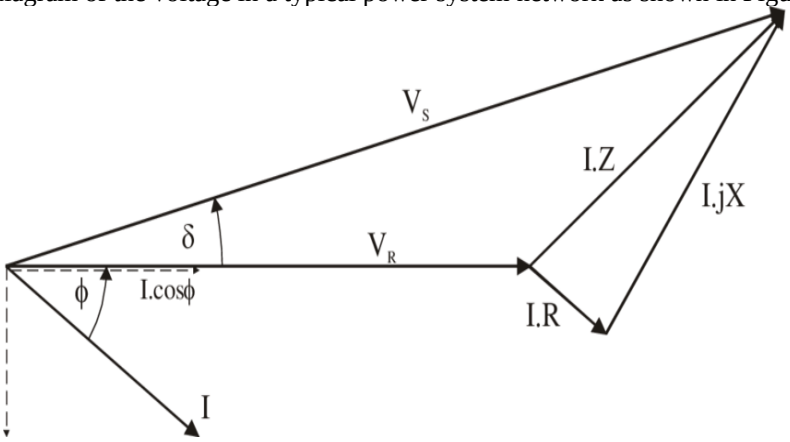


**Figure 1: Phasor Diagram of Voltage in a typical Power System Network (Muljadi et al., 2014)**

The drop in voltage on the feeder is given by;

$$|V_s - V_r| = |I(R_{LN} + jX_{LN})| \quad (6)$$

$$|V_s - V_r| = \left|\frac{(R_{LN}P_L + X_{LN}Q_L) - j(X_{LN}P_L - R_{LN}Q_L)}{V_r}\right| \quad (7)$$

For low power flow, the angle of voltage between the sending and receiving ends is minimal, allowing for an approximation of the voltage drop as shown thus;

$$|V_s - V_r| = \left|\frac{(R_{LN}P_L + X_{LN}Q_L)}{V_r}\right| \quad (8)$$

Three-phase voltages ($V_a$,$V_b$,$V_c$) are equal in magnitudes and interphase differently by 120°. These voltages are sequenced in the order a, b and c (positive sequence) if $V_b$ lags $V_a$ by 120° and $V_c$ lags $V_b$ by 120°. The three phasors can be described in terms of a reference $V_a$ thus;

$$V_a = V_a \quad (9)$$

$$V_b = \alpha^2 V_a \quad (10)$$

$$V_c = \alpha V_a \quad (11)$$

The complex number operator $\alpha$ is defined thus; $\alpha = e^{j120^o}$
Similarly, if the phase sequence is a, c and b (negative sequence) then;

$$V_a = V_a \quad (12)$$

$$V_b = \alpha V_a \quad (13)$$

$$V_c = \alpha^2 V_a \quad (14)$$

A set of balanced phasors is fully characterized by its reference phasor and its phase sequence (positive or negative)
Positive sequence phasors are written thus;

$$V_{a1} = V_{a1} \quad (15)$$

$$V_{b1} = \alpha^2 V_{a1} \quad (16)$$

$$V_{c1} = \alpha V_{a1} \quad (17)$$

Note the inclusion of the suffix 1
Negative sequences is written thus;

$$V_{a2} = V_{a2} \quad (18)$$
$$V_{b2} = \alpha V_{a2} \quad (19)$$
$$V_{c2} = \alpha^2 V_{a2} \quad (20)$$

That of zero sequence is written thus;

$$V_{a0} = V_{a0} \quad (21)$$
$$V_b = V_{a0} \quad (22)$$
$$V_c = V_{a0} \quad (23)$$

The three phasors can be expressed thus;

$$V_a = V_{a1} + V_{a2} + V_{a0} \quad (24)$$
$$V_b = \alpha^2 V_{a1} + \alpha V_{a2} + V_{a0} \quad (25)$$
$$V_c = \alpha V_{a1} + \alpha^2 V_{a2} + V_{a0} \quad (26)$$

The equations can be expressed in the form;

$$V_p = AV_s \quad (27)$$

Where

$V_p = \begin{bmatrix} V_a \\ V_b \\ V_c \end{bmatrix}$ = vector of original voltage phasors.

$V_s = \begin{bmatrix} V_{a1} \\ V_{a2} \\ V_{a0} \end{bmatrix}$ = vector of symmetrical components

$$A = \begin{bmatrix} 1 & 1 & 1 \\ \alpha^2 & \alpha & 1 \\ \alpha & \alpha^2 & 1 \end{bmatrix} \quad (28)$$

From Equation 27,

$$V_s = A^{-1}V_p \quad (29)$$

$$A^{-1} = \frac{1}{3}\begin{bmatrix} 1 & \alpha & \alpha^2 \\ 1 & \alpha^2 & \alpha \\ 1 & 1 & 1 \end{bmatrix} \quad (30)$$

In expanded form,

$$V_{a1} = \frac{1}{3}(V_a + \alpha V_b + \alpha^2 V_c) \quad (31)$$
$$V_{a2} = \frac{1}{3}(V_a + \alpha^2 V_b + \alpha V_c) \quad (32)$$
$$V_{a0} = \frac{1}{3}(V_a + V_b + V_c) \quad (33)$$

Figure 2 shows the graphical representation of the symmetrical components of phasor voltages.

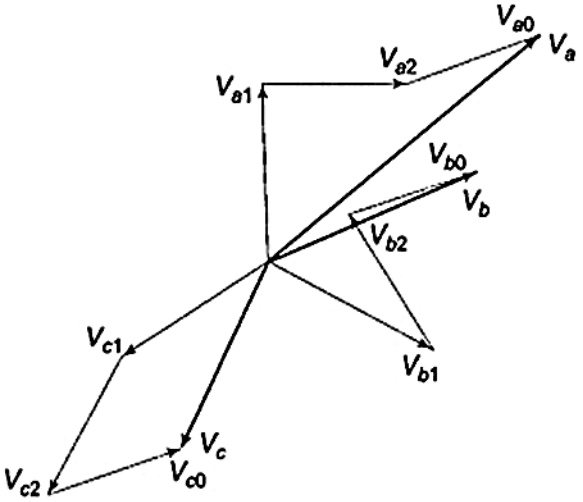


**Figure 2: Symmetrical Components of the Phasor Voltage**.

The symmetrical component transformations though given in terms of voltages hold for any of the phasors and therefore apply to a set of currents.

$$I_p = AI_s \quad (34)$$

$$I_s = A^{-1}I_p \quad (35)$$

$I_p = \begin{bmatrix} I_a \\ I_b \\ I_c \end{bmatrix}$ = vector of original phasors.

$I_s = \begin{bmatrix} I_{a1} \\ I_{a2} \\ I_{a0} \end{bmatrix}$ = vector of symmetrical components

$$I_a = I_{a1} + I_{a2} + I_{a0} \quad (36)$$

$$I_b = \alpha^2 I_{a1} + \alpha I_{a2} + I_{a0} \quad (37)$$

$$I_c = \alpha I_{a1} + \alpha^2 I_{a2} + I_{a0} \quad (38)$$

Obtaining the symmetrical component of the current phasor

$$I_{a1} = \frac{1}{3}(I_a + \alpha I_b + \alpha^2 I_c) \quad (39)$$

$$I_{a2} = \frac{1}{3}(I_a + \alpha^2 I_b + \alpha I_c) \quad (40)$$

$$I_{a0} = \frac{1}{3}(I_a + I_b + I_c) \quad (41)$$

### 2.1.1 Mathematical Analysis of Shunt Faults

Figure 3 shows a typical shunt fault.

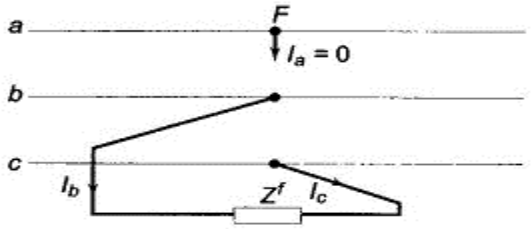


**Figure 3: Line to Line Fault (Shunt fault)**

The matrix representation of the current in line-to-line fault (between lines b and c) can be shown thus;

$$I_p = \begin{bmatrix} I_a = 0 \\ I_b \\ I_c = -I_b \end{bmatrix}; V_b - V_c = I_b Z^f$$

$Z^f$ is the fault impedance occurring through lines b and c.

The symmetrical components of the fault current are;

$$\begin{bmatrix} I_{a1} \\ I_{a2} \\ I_{a0} \end{bmatrix} = \frac{1}{3}\begin{bmatrix} 1 & \alpha & \alpha^2 \\ 1 & \alpha^2 & \alpha \\ 1 & 1 & 1 \end{bmatrix}\begin{bmatrix} 0 \\ I_b \\ -I_b \end{bmatrix} \quad (42)$$

From Equation (43);

$$I_{a2} = -I_{a1} \quad (43)$$

$$I_{a0} = 0 \quad (44)$$

The symmetrical components of voltages at fault are

$$\begin{bmatrix} V_{a1} \\ V_{a2} \\ V_{a0} \end{bmatrix} = \frac{1}{3}\begin{bmatrix} 1 & \alpha & \alpha^2 \\ 1 & \alpha^2 & 1 \\ 1 & 1 & 1 \end{bmatrix}\begin{bmatrix} V_a \\ V_b \\ V_b - Z^f I_b \end{bmatrix} \quad (45)$$

From Eq. (45),

$$3V_{a1} = V_a + (\alpha + \alpha^2)V_b - \alpha^2 Z^f I_b \quad (46)$$

$$3V_{a2} = V_a + (\alpha + \alpha^2)V_b - \alpha Z^f I_b \quad (47)$$

Solving Equations (46) and (47) simultaneously;

$$3(V_{a1} - V_{a2}) = (\alpha - \alpha^2)Z^f I_b = j\sqrt{3}Z^f I_b \quad (48)$$

The stages of the fault current are the sub-transient, transient, and steady-state. They occur for 0.5, 1.5-4 and over 30 cycles respectively.

**2.2 Simulation Parameters**

The parameters used in the simulation are contained in Table 1.

**Table 1: Parameters Used for Simulation**

| S/No. | Parameter | Value |
|---|---|---|
| 1 | Total buses used | 43 |
| 2 | Generator buses | 18 |
| 3 | Swing buses | 7 |
| 4 | Voltage Control Buses | 11 |
| 5 | Load Buses | 25 |
| 6 | Number of branches | 63 |
| 7 | Rated Line Voltage | 330kV |
| 8 | Load Flow Technique Adopted | Fast Decoupled Load Flow Technique (FDLF) |
| 9 | Maximum Iterations | 9999 |
| 10 | Precision | 0.01 |
| 11 | Critical Bus Voltage (Over Voltage) | 105% |
| 12 | Marginal Bus Voltage (Over Voltage) | 102% |
| 13 | Critical Bus Voltage (Under Voltage) | 95% |
| 14 | Marginal Bus Voltage (Under Voltage) | 98% |
| 16 | Marginal Generator Over excitation | 95% $Q_{max}$ |
| 17 | Load Demand (MW) | 3148.728 |
| 18 | Load Demand (MVAr) | 2583.736 |
| 19 | Generation (MW) | 3148.728 |
| 20 | Generation (MVAr) | 2583.736 |

**3.0 Results and Discussions**

The load flow study was done using a fast decoupled load flow technique and convergence was reached after three iterations. Table 2 shows details of the buses in critical conditions.

**Table 2: Load Flow Critical Report**

| S/No. | Buses | Bus Type | Status | Power Rating/Voltage Limit | Unit | Operating Condition | % Operating |
|---|---|---|---|---|---|---|---|
| 1 | Omoku Gas | Generator | Overload | 67.2 | MW | 67.2 | 100.0 |
| 2 | Gombe | Load Bus | Under Voltage | 330.0 | kV | 216.4 | 65.6 |
| 3 | Kainji hydro | Generator | Under Power | 0.0 | MW | -113.8 | 0.0 |
| 4 | Jebba hydro2 | Generator | Over Excited | 210.9 | Mvar | 812.5 | 385.2 |
| 5 | Jebba hydro2 | Generator | Overload | 500.0 | MW | 549.1 | 109.8 |
| 6 | Shiroro hydro4 | Generator | Overload | 500.0 | MW | 500.0 | 100.0 |
| 7 | Shiroro hydro4 | Generator | Under Excited | 0.0 | Mvar | 0.0 | 0.0 |
| 8 | Ih.Gas | Generator | Under Utilized | - | MW | -552.3 | - |
| 9 | Jalingo | Load Bus | Under Voltage | 330.0 | kV | 216.4 | 65.6 |
| 10 | Jos | Load Bus | Under Voltage | 330.0 | kV | 232.5 | 70.5 |
| 11 | Kaduna | Load Bus | Under Voltage | 330.0 | kV | 260.7 | 79.0 |
| 12 | Kano | Load Bus | Under Voltage | 330.0 | kV | 184.3 | 55.8 |
| 13 | Maidugiri | Load Bus | Under Voltage | 330.0 | kV | 216.4 | 65.6 |

| | | | | | | | |
|---|---|---|---|---|---|---|---|
| 14 | NIPP | Generator | Overload | 500.0 | MW | 500.0 | 100.0 |
| 15 | NIPP | Generator | Under Excited | - | Mvar | - | - |
| 16 | NIPP I | Generator | Under Excited | 0.0 | Mvar | 0.0 | 0.0 |
| 17 | NIPP I | Generator | Overload | 750.0 | MW | 750.0 | 100.0 |
| 18 | O.Gas | Generator | Overload | 67.4 | MW | 67.4 | 100.0 |
| 19 | O.Gas | Generator | Under Excited | 0.0 | Mvar | 0.0 | 0.0 |
| 20 | O.Gas. | Generator | Under Excited | 0.0 | Mvar | 0.0 | 0 |
| 21 | O.Gas. | Generator | Overload | 378.0 | MW | 378.0 | 100 |
| 22 | O.NIPP | Generator | Overload | 100.0 | MW | 100.0 | 100 |
| 23 | O.NIPP | Generator | Under Excited | 0.0 | MVAr | 0.0 | 0.0 |
| 24 | Olorunsogo | Load Bus | Under Voltage | 330.0 | kV | 313.1 | 94.8 |
| 25 | Osogbo | Load Bus | Under Voltage | 330.0 | kV | 312.7 | 94.7 |
| 26 | Steam | Generator | Overload | 336.9 | MW | 336.9 | 100.0 |
| 27 | Steam | Generator | Under Excited | 0.0 | MVAr | 0.0 | 0.0 |
| 28 | Yola | Load Bus | Under Voltage | 330.0 | kV | 216.4 | 65.5 |

From Table 2, three overloaded buses, viz. Jebba Hydro, Shiroro Hydro, and Olorunsogo Gas were selected alongside two undervolted buses (Yola and Maiduguri buses).
Table 3 provides details of the total generation, loading and demand of the network

**Table 3: The Total Generation, Loading and Demand of the Network**

| | MW | MVAr | MVA | % PF Lagging |
|---|---|---|---|---|
| Power Generation (Slack Buses): | 69.42 | 2583.74 | 2584.67 | 2.69 |
| Source (Non-Slack Buses): | 3079.31 | 0.00 | 3079.31 | 100.00 |
| Total Demand: | 3148.73 | 2583.74 | 4073.10 | 77.31 |
| Total Motor Load: | 2540.95 | 1574.74 | 2989.35 | 85.00 |
| Total Static Load: | 526.64 | 326.38 | 619.57 | 85.00 |
| Apparent Losses: | 81.14 | 682.62 | - | - |
| System Mismatch: | 0.12 | 0.00 | - | - |

Table 4 gives the sub-transient cycle (1/2 Cycle) result for the short circuit analysis on the Jebba hydro generating station.

**Table 4: Short-Circuit Summary Report for Jebba GS**

| | | 3-Phase Fault Current (kA) | | | Line-to-Ground Fault Current (kA) | | | Line-to-Line Fault Current (kA) | | | Line-to-Line-to-Ground Current (kA) | | |
|---|---|---|---|---|---|---|---|---|---|---|---|---|---|
| Bus | kV | Real Component | Imag. Component | Current Mag. | Real Component | Imag. Component | Current Mag. | Real Component | Imag. Component | Current Mag. | Real Component | Imag. Component | Current Mag. |
| Jebba GS | 330 | 1.22 | -14.30 | 14.35 | 1.83 | -15.47 | 15.58 | 12.52 | 1.24 | 12.58 | -13.51 | 7.05 | 15.24 |

The line-to-ground fault exhibited the highest current magnitude at 15.58 kA, while the line-to-line fault recorded the lowest at 12.58 kA. The magnitude of the 3-phase fault, line-to-ground fault and line-to-line fault are $14.35e^{-j85.23^o}$, $15.58e^{-j83.18^o}$ and $15.24e^{j152.4^o}$ respectively.

Table 5 gives the sub-transient cycle result (voltages) for the short circuit analysis on the Jebba hydro generating station.

**Table 5: Symmetrical Component of the Phasor Voltage from Jebba GS**

| Buses | | 3-Phase Fault | | Line-To-Ground Fault | | | | |
|---|---|---|---|---|---|---|---|---|
| | | % V | kA | % Voltage at Sending Bus | | | kA Symm. rms | |
| Sending Bus | Receiving Bus | From Bus | Symm. Rms | Va | Vb | Vc | Ia | 3I0 |
| Jebba GS | Total | 0.00 | 14.35 | 0.00 | 94.52 | 97.38 | 15.58 | 15.58 |
| Jebba | Jebba GS | 5.74 | 4.47 | 6.38 | 94.53 | 97.25 | 3.73 | 1.56 |
| Jebba | Jebba GS | 5.74 | 4.47 | 6.38 | 94.53 | 97.25 | 3.73 | 1.56 |
| hydro4 | Jebba GS | 100.00 | 5.41 | 100.00 | 100.00 | 100.00 | 8.12 | 12.48 |

Note that 3I0 represents the current in the neutral line.
Table 6 gives the sub-transient cycle (1/2 cycle) result for the short circuit analysis on Shiroro hydro generating station.

**Table 6: Report on the Short-Circuit Fault at Shiroro GS**

| | | 3-Phase Fault current (kA) | | | Line-to-Ground Fault current (kA) | | | Line-to-Line Fault current (kA) | | | Line-to-Line-to-Ground current (kA) | | |
|---|---|---|---|---|---|---|---|---|---|---|---|---|---|
| Buses | Line Voltage(kV) | Real Current | Imag. Component | Current Mag. | Real Current | Imag. Component | Current Mag. | Real current | Imag. component | Current Mag. | Real Current | Imag. Component | Current Mag. |
| Shiroro GS | 330 | 1.07 | -12.53 | 12.58 | 1.55 | -13.55 | 13.64 | 10.97 | 1.08 | 11.02 | -11.78 | 6.19 | 13.31 |

The line-to-ground fault had the highest fault current at 13.64 kA. The line-to-line fault had the lowest fault current at 11.02 kA. The magnitudes of the faults are: $12.58e^{-j84.9^o}$, $13.64e^{-j83.41^o}$ and $11.02e^{j5.6^o}$ respectively.
Table 7 gives the sub-transient cycle result (voltages) for the short circuit analysis on Shiroro hydro generating station.

Table 7. Symmetrical Component of the Phasor Voltage for Shiroro GS

| Buses | | Fault at 3-Phase | | Line-To-Ground Fault | | | | |
|---|---|---|---|---|---|---|---|---|
| Sending Bus | Receiving Bus | % V From Bus | kA Symm. RMS | % Voltage at Sending Bus | | | kA Symm. RMS | |
| | | | | Va | Vb | Vc | Ia | 3I0 |
| Shiroro GS | Total | 1.1E-14 | 12.58 | 5.6E-15 | 94.88 | 97.11 | 13.64 | 13.64 |
| Kaduna | Shiroro GS | 4.2E+01 | 2.47 | 3.0E+01 | 102.70 | 104.73 | 1.77 | 0.00 |
| Kaduna II | Shiroro GS | 1.1E-14 | 0.00 | 6.1E-15 | 94.88 | 97.11 | 0.00 | 0.00 |
| Jebba | Shiroro GS | 8.3E+01 | 2.07 | 8.7E+01 | 97.71 | 97.68 | 1.70 | 0.66 |
| Gwaggwalada | Shiroro GS | 2.7E+01 | 1.36 | 2.6E+01 | 96.86 | 98.48 | 1.08 | 0.31 |
| Katampe | Shiroro GS | 2.5E+01 | 1.27 | 2.2E+01 | 97.48 | 99.31 | 0.98 | 0.21 |
| Kaduna I | Shiroro GS | 1.1E-14 | 0.00 | 6.1E-15 | 94.88 | 97.11 | 0.00 | 0.00 |
| hydro2 | Shiroro GS | 1.0E+02 | 5.41 | 1.0E+02 | 100.00 | 100.00 | 8.12 | 12.47 |

Table 8 gives the sub-transient cycle result for the short circuit analysis on Olorunsogo generating station.

**Table 8: Report on the Short-Circuit Fault at Olorunsogo GS**

| | | 3-Phase current Fault (kA) | | | Line-to-Ground current Fault (kA) | | | Line-to-Line Fault current (kA) | | | *Line-to-Line-to-Ground (kA) | | |
|---|---|---|---|---|---|---|---|---|---|---|---|---|---|
| Buses | kV | Real component | Imag. component | Current Mag. | Real component | Imag. component | Current Mag. | Real Component | Imag. Component | Current Mag. | Real | Imag. | Mag. |
| Olorunsogo | 330 | 1.41 | -17.41 | 17.47 | 2.20 | -19.76 | 19.88 | 15.26 | 1.47 | 15.33 | -16.45 | 9.74 | 19.12 |

The line-to-ground fault current reached its peak with a magnitude of 19.88 kA, making it the highest among the various fault types. In contrast, the line-to-line fault exhibited the lowest fault current magnitude at 15.33 kA. The magnitudes for the three-phase fault, line-to-ground fault, and line-to-line fault stand at $17.47e^{-j85.25^o}$, $19.88e^{-j83.70^o}$ and $15.33e^{j5.5^o}$ respectively.

Table 9 gives the sub-transient cycle result (voltages) for the short circuit analysis on Olorunsogo hydro generating station.

**Table 9: Symmetrical Component of the Phasor Voltage for Olorunsogo GS**

| Buses | | 3-Phase Current Fault | | Line-To-Ground Current Fault | | | | |
|---|---|---|---|---|---|---|---|---|
| Sending Bus | Receiving Bus | % V From Bus | kA Symm. Rms | % Voltage at From Bus | | | kA Symm. RMS | |
| | | | | Va | Vb | Vc | Ia | 3I0 |
| Olorunsogo | Total | 0.00 | 17.46 | 0.00 | 92.62 | 94.77 | 19.88 | 19.88 |
| Ikeja West | Olorunsogo | 66.60 | 4.94 | 68.53 | 96.73 | 97.00 | 4.16 | 1.35 |
| Ayede | Olorunsogo | 38.71 | 3.69 | 35.12 | 96.87 | 98.41 | 2.95 | 0.57 |
| Gas | Olorunsogo | 100.00 | 0.73 | 100.00 | 100.00 | 100.00 | 1.05 | 1.48 |
| NIPP 1 | Olorunsogo | 100.00 | 8.11 | 100.00 | 100.00 | 100.00 | 11.72 | 16.49 |

Table 10 gives the sub-transient cycle (1/2 cycle) result for the short circuit analysis on bus Yola.

**Table 10: Report on the Short-Circuit Fault at Bus Yola**

| | | 3-Phase Current Fault (kA) | | | Line-to-Ground Current Fault (kA) | | | Line-to-Line Current Fault (kA) | | | *Line-to-Line-to-Ground Current (kA) | | |
|---|---|---|---|---|---|---|---|---|---|---|---|---|---|
| Bus | kV | Real component | Imag. | Mag. | Real Component | Imag. | Mag. | Real | Imag. | Mag. | Real | Imag. | Mag. |
| Yola | 330 | 0.12 | -1.03 | 1.04 | 0.11 | -0.47 | 0.48 | 0.89 | 0.10 | 0.90 | -0.93 | 0.05 | 0.94 |

The 3-phase fault results in the highest fault current, measuring at 1.04 kA. Conversely, the line-to-ground fault records the lowest current at 0.48 kA. The fault current magnitudes for the 3-phase fault, line-to-ground fault, and line-to-line fault are $1.04e^{-j82.05^o}$, $0.48e^{-j78.28^o}$ and $0.9e^{j6.38^o}$ respectively.

Table 11 gives the sub-transient cycle result (voltages) for the short circuit analysis on bus Yola.

**Table 11: Symmetrical Component of the Phasor Voltage for Bus Yola**

| Contribution | | 3-Phase Fault | | Line-To-Ground Fault | | | | |
|---|---|---|---|---|---|---|---|---|
| From Bus | To Bus | % V From Bus | kA Symm. Rms | % Voltage at From Bus | | | kA Symm. rms | |
| | | | | Va | Vb | Vc | Ia | 3I0 |
| Yola | Total | 0.00 | 1.04 | 0.00 | 132.26 | 138.73 | 0.48 | 0.48 |
| Gombe | Yola | 43.64 | 1.04 | 33.93 | 122.79 | 127.39 | 0.48 | 0.48 |
| Jalingo | Yola | 0.00 | 0.00 | 0.00 | 132.26 | 138.73 | 0.00 | 0.00 |

Table 12 gives the sub-transient cycle result for the short circuit analysis on the bus Maiduguri.

**Table 12: Report on the Short-Circuit Fault at Bus Maiduguri**

| | | 3-Phase Current Fault (kA) | | | Line-to-Ground Current Fault (kA) | | | Line-to-Line Current Fault (kA) | | | *Line-to-Line-to-Ground Current (kA) | | |
|---|---|---|---|---|---|---|---|---|---|---|---|---|---|
| Bus | kV | Real Component | Imag. Component | Mag. | Real | Imag. | Mag. | Real | Imag. | Mag. | Real | Imag. | Mag. |
| Maidugiri | 330 | 0.09 | -0.78 | 0.78 | 0.08 | -0.37 | 0.38 | 0.67 | 0.08 | 0.68 | -0.71 | 0.04 | 0.71 |

The 3-phase fault showed the highest current at 0.78 kA. The line-to-ground fault had the lowest current at 0.38 kA. The currents for the 3-phase fault, line-to-ground fault, and line-to-line fault are $0.78e^{-j90^o}$, $0.38e^{-j76.82^o}$ and $0.68e^{j6.76^o}$ respectively.

Table 13 gives the sub-transient cycle result (voltages) for the short circuit analysis on bus Maiduguri.

**Table 13: Symmetrical Component of the Phasor Voltage for Bus Maiduguri**

| Buses | | 3-Phase Voltage/Current Fault | | Line-To-Ground Fault | | | | |
|---|---|---|---|---|---|---|---|---|
| Sending Bus | Receiving Bus | % V From Bus | kA Symm. Rms | % Voltage at From Bus | | | kA Symm. RMS | |
| | | | | Va | Vb | Vc | Ia | 3I0 |
| Maidugiri | Total | 0.00 | 0.78 | 0.00 | 130.07 | 136.82 | 0.38 | 0.38 |
| Damaturu | Maidugiri | 35.62 | 0.78 | 29.30 | 121.98 | 127.08 | 0.38 | 0.38 |

The voltage stability in the five buses (Jebba Hydro, Shiroro Hydro, Olorunsogo gas, Yola bus and Maiduguri bus) was analysed using transient stability analysis.

The rotor angle of the Jebba hydro generator was examined during a transient fault that occurred in the network between 0.75 seconds and 1.1 seconds. Figure 4 graphically illustrates the generator behaviour.

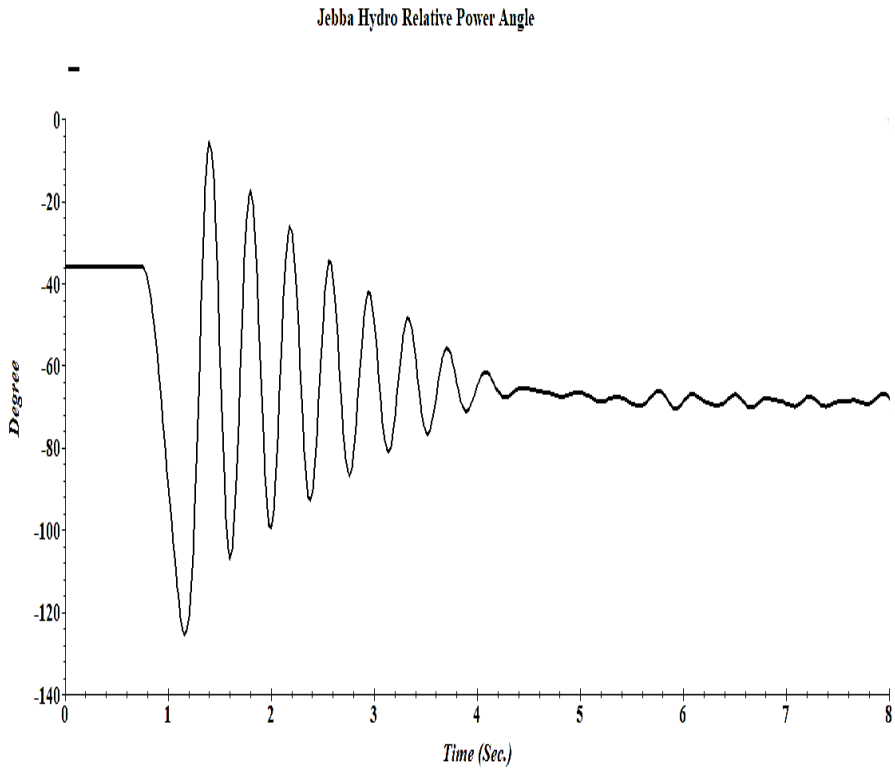


**Figure 4: Jebba Hydro Generator Relative Power Angle**

The fault was cleared at 1.1 sec, but the generator rotor angle kept swinging, hence unstable.
The VAr compensator was introduced at the bus Jebba hydro generator and the rotor angle stabilized.
Figure 5. illustrates the extent of stability.

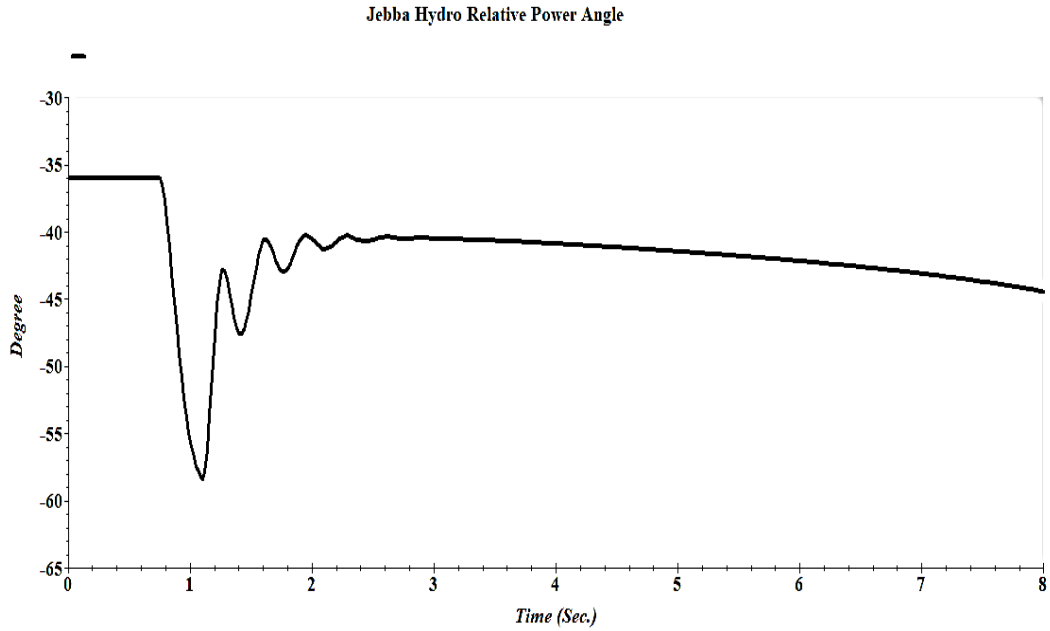


**Figure 5: Jebba Hydro Generator Rotor Angle after Compensation**

The rotor angle of the Shiroro hydro generator was studied when a transient fault was introduced into the network at 0.75 sec and lasted till 1.1 sec. Figure 6. graphically illustrates the behaviour of the generator.

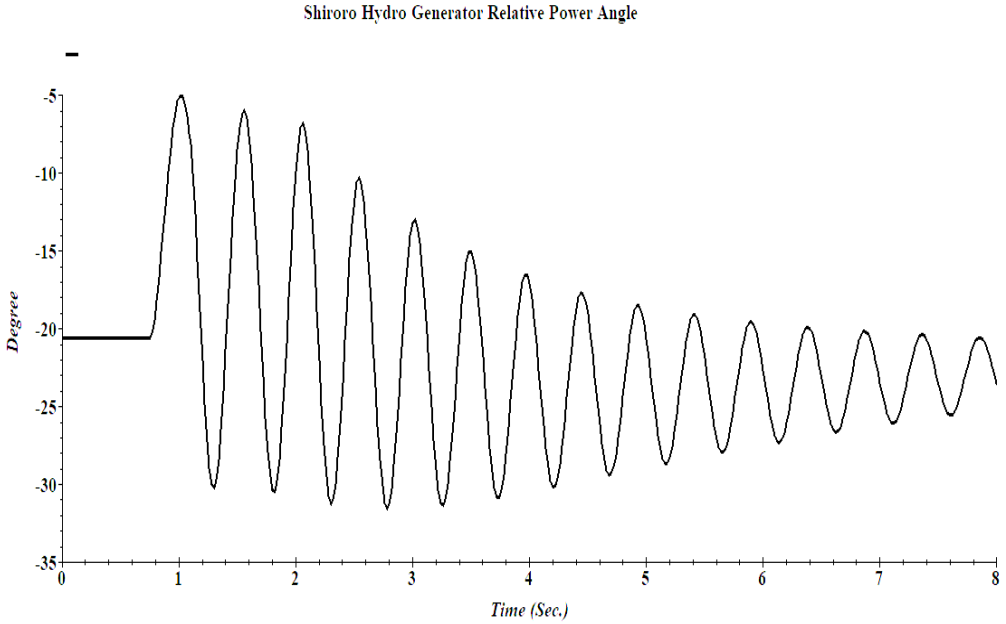


**Figure 6: Shiroro Hydro Generator Relative Power Angle**

The fault was cleared at 1.1 sec, but the generator rotor angle kept oscillating, hence unstable. The VAr compensator was introduced at bus Shiroro hydro generator and the rotor angle stabilized. Figure 7. illustrates the extent of stability.

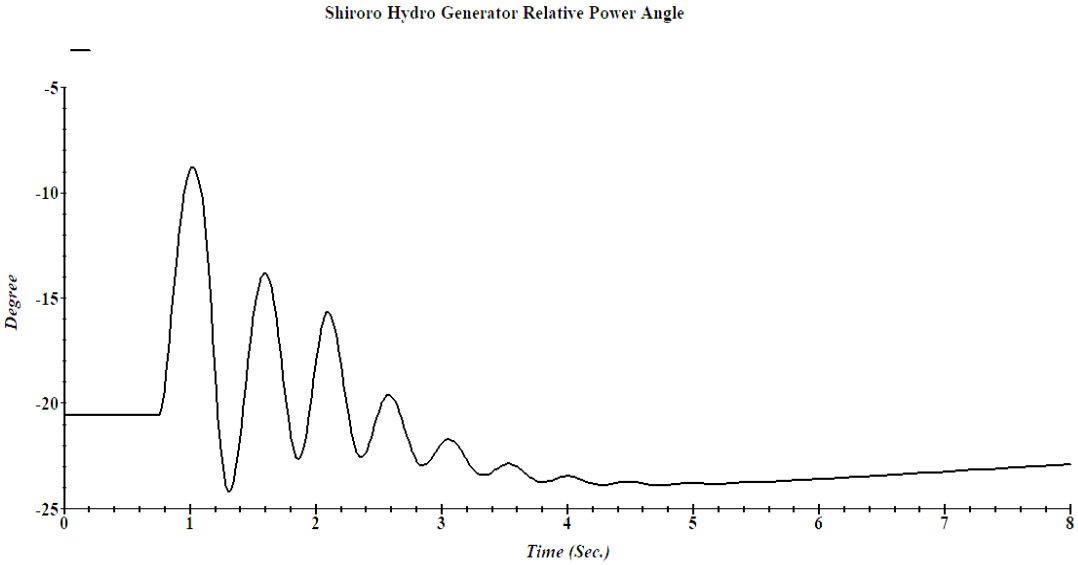


**Figure 7: Shiroro Hydro Generator Relative Power Angle after Compensation**

The rotor angle of Olorunsogo generator was studied when a transient fault was introduced into the network at 0.75 sec and lasted till 1.1 sec. Figure 8. shows graphically, the behaviour of the generator.

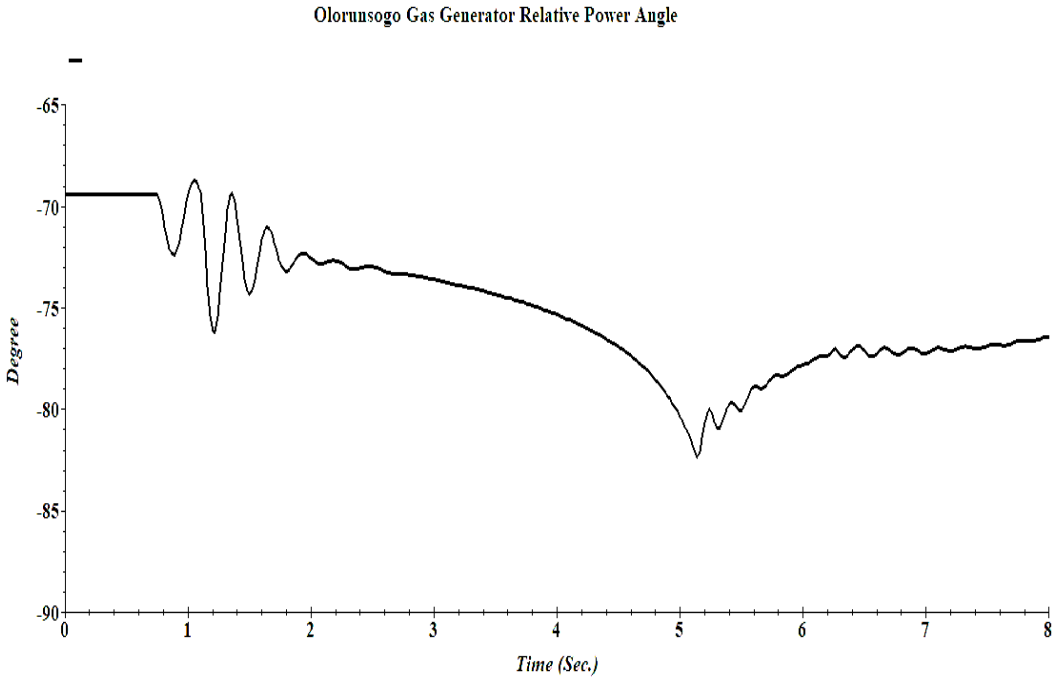


**Figure 8: Olorunsogo Gas Generator Relative Power Angle**

The fault was cleared at 1.1 sec, but the generator rotor angle kept oscillating, hence unstable.
The VAr compensator was introduced at bus Olorunsogo gas generator and the rotor angle stabilized.
Figure 9. illustrates the extent of stability

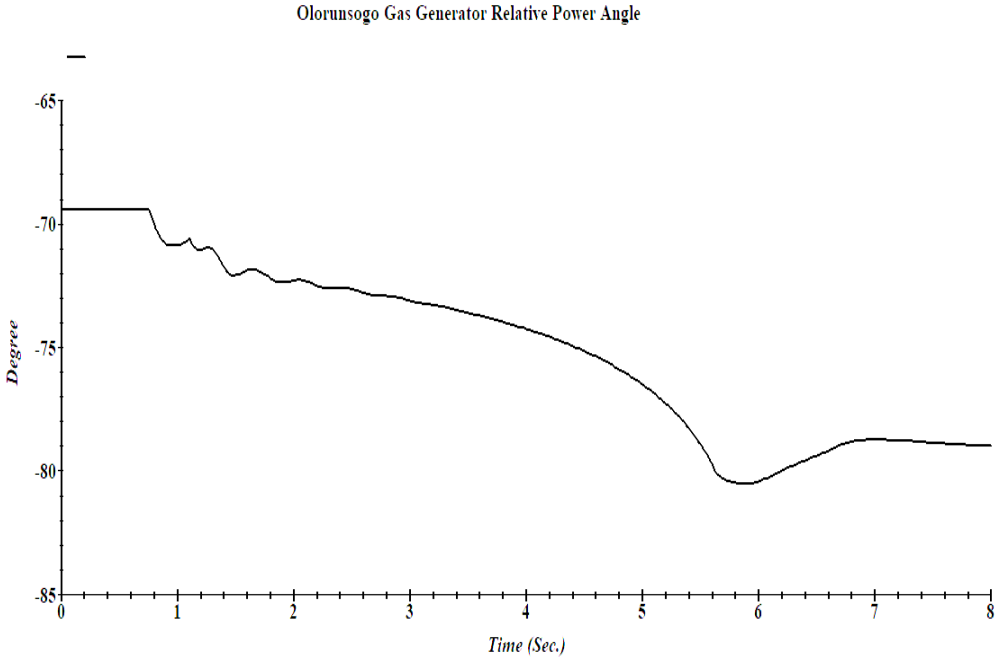


**Figure 9: Olorunsogo Gas Generator Relative Power Angle after Compensation**

Figure 10. represents the voltage magnitude for the buses before and after compensation.

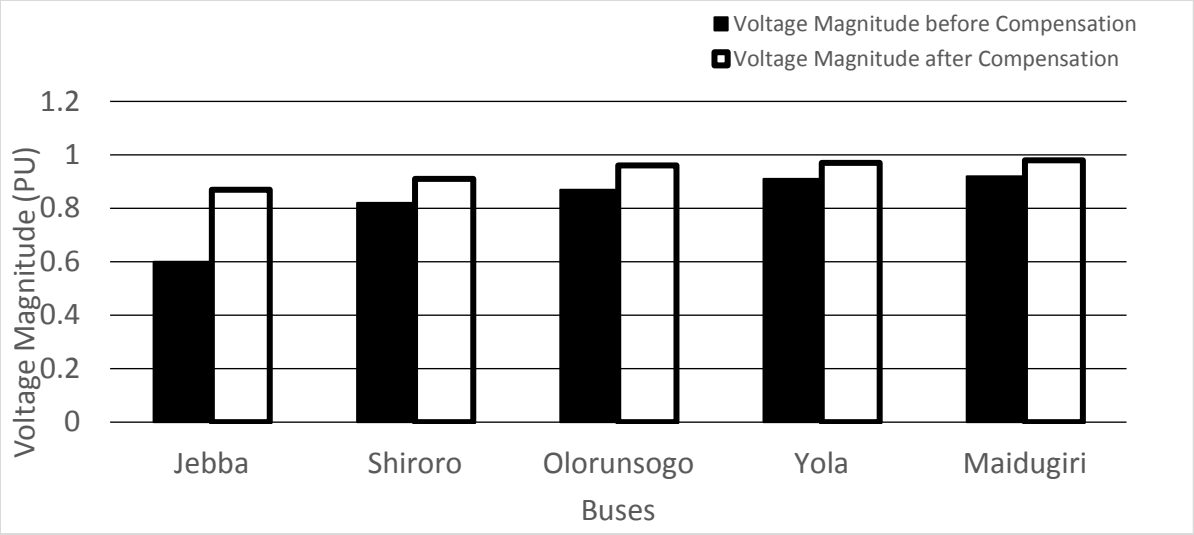


**Figure 10: Voltage Magnitude for the Buses before and after Compensation**

It can be seen that with the introduction of VAr devices at the defective buses, there was an improvement in the voltage magnitude.

## 4.0. Conclusion

This work presented the voltage stability study of the 330 kV grid network of Nigeria. The power flow in the grid network was studied to obtain the status of each bus in the network. From this study, critical and marginal buses were identified. Shunt faults were introduced to the critical buses and the sub-transient cycles of the faults were studied. Three-phase fault current was the highest of all other fault currents. Voltage stability on buses was also studied by conducting a transient stability assessment using adaptive Newton Raphson's technique. A reactive power source (VAr source) was introduced to the network and its effect on the voltages of the buses was observed. An improvement in voltage magnitude was observed after the introduction of the VAr source.

## 5.0 Recommendation

The Nigerian Transmission Company (TCN) and distribution companies should consider implementing reactive power compensation devices such as VAr sources at critical buses to improve voltage stability and reduce the risk of power system collapse.

## References

Abdalla Seedahmed, M. M., Sofyan Mokred, S. A., & Kamara, G. 2019. Voltage Stability Estimation for Complex Power System Based on Modal Analytical Techniques. *2019 6th International Conference on Signal Processing and Integrated Networks, SPIN 2019*. https://doi.org/10.1109/SPIN.2019.8711683

Abdukhakimov, A., Bhardwaj, S., Gashema, G., & Kim, D. S. 2019. Reliability analysis in smart grid networks considering distributed energy resources and storage devices. *International Journal of Electrical and Electronic Engineering and Telecommunications*, *8*(5). https://doi.org/10.18178/ijeetc.8.5.233-237

Adebayo, I., & Sun, Y. 2017. New performance indices for voltage stability analysis in a power system. *Energies*, *10*(12). https://doi.org/10.3390/en10122042

Adegoke, S. A., & Sun, Y. 2023. Power system optimization approach to mitigate voltage instability issues: A review. In *Cogent Engineering* (Vol. 10, Issue 1). https://doi.org/10.1080/23311916.2022.2153416

Adoghe, A. U., Adeyemi-Kayode, T. M., Oguntosin, V., & Amahia, I. I. 2023. Performance evaluation of the prospects and challenges of effective power generation and distribution in Nigeria. In *Heliyon* (Vol. 9, Issue 3). https://doi.org/10.1016/j.heliyon.2023.e14416

Alimi, O. A., Ouahada, K., & Abu-Mahfouz, A. M. 2020. A Review of Machine Learning Approaches to Power System Security and Stability. In *IEEE Access* (Vol. 8). https://doi.org/10.1109/ACCESS.2020.3003568

Aminifar, F., Rahmatian, F., & Shahidehpour, M. 2021. State-of-the-Art in Synchrophasor Measurement Technology Applications in Distribution Networks and Microgrids. *IEEE Access*, *9*. https://doi.org/10.1109/ACCESS.2021.3127915

Amroune, M. 2021. Machine Learning Techniques Applied to On-Line Voltage Stability Assessment: A Review. *Archives of Computational Methods in Engineering*, *28*(2). https://doi.org/10.1007/s11831-019-09368-2

Bazrafshan, M., & Gatsis, N. 2018. Comprehensive Modeling of Three-Phase Distribution Systems via the Bus Admittance Matrix. *IEEE Transactions on Power Systems*, *33*(2). https://doi.org/10.1109/TPWRS.2017.2728618

Biswal, C., Sahu, B. K., Mishra, M., & Rout, P. K. 2023. Real-Time Grid Monitoring and Protection: A Comprehensive Survey on the Advantages of Phasor Measurement Units. In *Energies* (Vol. 16, Issue 10). https://doi.org/10.3390/en16104054

Blaabjerg, F., Yang, Y., Yang, D., & Wang, X. 2017. Distributed Power-Generation Systems and Protection. In *Proceedings of the IEEE* (Vol. 105, Issue 7). https://doi.org/10.1109/JPROC.2017.2696878

Bogodorova, T., Vanfretti, L., & Turitsyn, K. 2016. Voltage control-based ancillary service using thermostatically controlled loads. *IEEE Power and Energy Society General Meeting*, *2016-November*. https://doi.org/10.1109/PESGM.2016.7741640

Bu, S., Meegahapola, L. G., Wadduwage, D. P., & Foley, A. M. 2023. Stability and Dynamics of Active Distribution Networks (ADNs) With D-PMU Technology: A Review. *IEEE Transactions on Power Systems*, *38*(3). https://doi.org/10.1109/TPWRS.2022.3179488

Chintakindi, R., Pradhan, P., & Mitra, A. 2022. WAMS based Thevenin Index for voltage stability assessment with increasing wind power penetration and additional distributed load. *Energy Reports*, *8*. https://doi.org/10.1016/j.egyr.2021.11.215

Dada, J. O. 2014. Towards understanding the benefits and challenges of Smart/Micro-Grid for electricity supply system in Nigeria. In *Renewable and Sustainable Energy Reviews* (Vol. 38). https://doi.org/10.1016/j.rser.2014.07.077

Danish, M. S. S., Senjyu, T., Danish, S. M. S., Sabory, N. R., Narayanan, K., & Mandal, P. 2019. A recap of voltage stability indices in the past three decades. *Energies*, *12*(8). https://doi.org/10.3390/en12081544

Das, S., & Panigrahi, B. 2022. A PMU-Based Data-Driven Approach for Enhancing Situational Awareness in Building A Resilient Power Systems. *IEEE Transactions on Industrial Informatics*, *18*(7). https://doi.org/10.1109/TII.2022.3147794

Das, S. R., Mishra, D. P., Ray, P. K., Salkuti, S. R., & Sahoo, A. K. 2021. Power quality improvement using fuzzy logic-based compensation in a hybrid power system. *International Journal of Power Electronics and Drive Systems*, *12*(1). https://doi.org/10.11591/ijpeds.v12.i1.pp576-584

Gadal, R., Oukennou, A., El Mariami, F., Belfqih, A., & Agouzoul, N. 2023. Voltage Stability Assessment and Control Using Indices and FACTS: A Comparative Review. In *Journal of Electrical and Computer Engineering* (Vol. 2023). https://doi.org/10.1155/2023/5419372

Hamoud, G. A. 2023. Reliability Assessment of Distribution Power Transformers Considering Load Transfer Capability. *IEEE Transactions on Power Systems*, *38*(2). https://doi.org/10.1109/TPWRS.2022.3171693

Hay, S., & Ferguson, A. 2015. A Review of Power System Modelling Platforms and Capabilities. In *IET Special Interest Publication for the Council for Science and Technology*.

Hossain, M. A., Pota, H. R., Hossain, M. J., & Blaabjerg, F. 2019. Evolution of microgrids with converter-interfaced generations: Challenges and opportunities. In *International Journal of Electrical Power and Energy Systems* (Vol. 109). https://doi.org/10.1016/j.ijepes.2019.01.038

Hosseinzadeh, N., Aziz, A., Mahmud, A., Gargoom, A., & Rabbani, M. 2021. Voltage stability of power systems with renewable-energy inverter-based generators: A review. In *Electronics (Switzerland)* (Vol. 10, Issue 2). https://doi.org/10.3390/electronics10020115

Ismael, S. M., Abdel Aleem, S. H. E., Abdelaziz, A. Y., & Zobaa, A. F. 2019. State-of-the-art of hosting capacity in modern power systems with distributed generation. In *Renewable Energy* (Vol. 130). https://doi.org/10.1016/j.renene.2018.07.008

Ismail, B., Abdul Wahab, N. I., Othman, M. L., Radzi, M. A. M., Naidu Vijyakumar, K., & Mat Naain, M. N. 2020. A Comprehensive Review on Optimal Location and Sizing of Reactive Power Compensation Using Hybrid-Based Approaches for Power Loss Reduction, Voltage Stability Improvement, Voltage Profile Enhancement and Loadability Enhancement. *IEEE Access*, *8*. https://doi.org/10.1109/ACCESS.2020.3043297

Jiang, Y., & Meng, X. 2023. A battery capacity estimation method based on the equivalent circuit model and quantile regression using vehicle real-world operation data. *Energy*, *284*. https://doi.org/10.1016/j.energy.2023.129126

Jimoh, M. A., & Raji, B. 2023. Electric Grid Reliability: An Assessment of the Nigerian Power System Failures, Causes and Mitigations. *Covenant Journal of Engineering Technology*, *7*(1).

Kasar, A. B., Budania, R., & Sarwade, A. 2024. Nanotechnology Perceptions ISSN 1660-6795 www. In *Nanotechnology Perceptions* (Vol. 20, Issue S11). www.nano-ntp.com

Lee, Y., & Han, S. 2019. Real-time voltage stability assessment method for the Korean power system based on estimation of Thévenin equivalent impedance. *Applied Sciences (Switzerland)*, *9*(8). https://doi.org/10.3390/app9081671

Lee, Y., & Song, H. 2019. A reactive power compensation strategy for voltage stability challenges in the Korean power system with dynamic loads. *Sustainability (Switzerland)*, *11*(2). https://doi.org/10.3390/su11020326

Liang, X., Chai, H., & Ravishankar, J. 2022. Analytical Methods of Voltage Stability in Renewable Dominated Power Systems: A Review. In *Electricity* (Vol. 3, Issue 1). https://doi.org/10.3390/electricity3010006

Liu, W., Kerekes, T., Dragicevic, T., & Teodorescu, R. 2023. Review of Grid Stability Assessment Based on AI and a New Concept of Converter-Dominated Power System State of Stability Assessment. *IEEE Journal of Emerging and Selected Topics in Industrial Electronics*, *4*(3). https://doi.org/10.1109/jestie.2023.3236885

Madueme, T. C., & Onyegbadue, I. A. 2018. *Application of UPFC for optimization of the Nigeria application of UPFC for optimization of the Nigeria*. http://www.casirmediapublishing.comhttp://www.casirmediapublishing.comhttp://www.casirmediapublishing.comhttp://www.casirmediapublishing.com

Malik, F. H., Khan, M. W., Rahman, T. U., Ehtisham, M., Faheem, M., Haider, Z. M., & Lehtonen, M. 2024. A Comprehensive Review on Voltage Stability in Wind-Integrated Power Systems. In *Energies* (Vol. 17, Issue 3). https://doi.org/10.3390/en17030644

Massaoudi, M. S., Abu-Rub, H., & Ghrayeb, A. 2023. Navigating the Landscape of Deep Reinforcement Learning for Power System Stability Control: A Review. *IEEE Access*, *11*. https://doi.org/10.1109/ACCESS.2023.3337118

Mehigan, L., Deane, J. P., Gallachóir, B. P. Ó., & Bertsch, V. 2018. A review of the role of distributed generation (DG) in future electricity systems. In *Energy* (Vol. 163). https://doi.org/10.1016/j.energy.2018.08.022

Modarresi, J., Gholipour, E., & Khodabakhshian, A. 2016. A comprehensive review of the voltage stability indices. In *Renewable and Sustainable Energy Reviews* (Vol. 63). https://doi.org/10.1016/j.rser.2016.05.010

Moheb, A. M., El-Hay, E. A., & El-Fergany, A. A. 2022. Comprehensive Review on Fault Ride-Through Requirements of Renewable Hybrid Microgrids. In *Energies* (Vol. 15, Issue 18). https://doi.org/10.3390/en15186785

Mokred, S., & Wang, Y. 2024. Voltage stability assessment and contingency ranking in power systems based on modern stability assessment index. *Results in Engineering*, *23*. https://doi.org/10.1016/j.rineng.2024.102548

Montoya, O. D., Giraldo, J. S., Grisales-Noreña, L. F., Chamorro, H. R., & Alvarado-Barrios, L. 2021. Accurate and efficient derivative-free three-phase power flow method for unbalanced distribution networks. *Computation*, *9*(6). https://doi.org/10.3390/computation9060061

Monyei, C. G., Adewumi, A. O., Obolo, M. O., & Sajou, B. 2018. Nigeria's energy poverty: Insights and implications for smart policies and framework towards a smart Nigeria electricity network. In *Renewable and Sustainable Energy Reviews* (Vol. 81). https://doi.org/10.1016/j.rser.2017.05.237

Muhtadi, A., Pandit, D., Nguyen, N., & Mitra, J. 2021. Distributed Energy Resources Based Microgrid: Review of Architecture, Control, and Reliability. *IEEE Transactions on Industry Applications*, *57*(3). https://doi.org/10.1109/TIA.2021.3065329

Muljadi, E., Singh, M., & Gevorgian, V. 2014. User Guide for PV Dynamic Model Simulation Written on PSCAD Platform. *NREL*.

Muthulakshmi, K., Sasiraja, R. M., & Suresh Kumar, V. 2017. The proper location and sizing of multiple distributed generators for maximizing voltage stability using PSO. *Journal of Circuits, Systems and Computers*, *26*(4). https://doi.org/10.1142/S0218126617500578

Nageswa Rao, A. R., Vijaya, P., & Kowsalya, M. 2021. Voltage stability indices for stability assessment: a review. In *International Journal of Ambient Energy* (Vol. 42, Issue 7). https://doi.org/10.1080/01430750.2018.1525585

Neves, L., & Alberto, L. 2021. *On The Computation of The Locally Closest Bifurcation Point Considering Loading Uncertainties and Reactive Power Limits*. https://doi.org/10.1109/pesgm46819.2021.9637849

Neves, L. S., & Costa Alberto, L. F. 2020. On the Computation of the Locally Closest Bifurcation Point Considering Loading Uncertainties and Reactive Power Limits. *IEEE Transactions on Power Systems*, *35*(5). https://doi.org/10.1109/TPWRS.2020.2976191

Nguyen Duc, H., Kamwa, I., Dessaint, L. A., & Cao-Duc, H. 2017. A novel approach for early detection of impending voltage collapse events based on the support vector machine. *International Transactions on Electrical Energy Systems*, *27*(9). https://doi.org/10.1002/etep.2375

Nirbhavane, P. S., Corson, L., Rizvi, S. M. H., & Srivastava, A. K. 2021. TPCPF: Three-Phase Continuation Power Flow Tool for Voltage Stability Assessment of Distribution Networks with Distributed Energy Resources. *IEEE Transactions on Industry Applications*, *57*(5). https://doi.org/10.1109/TIA.2021.3088384

Okampo, E. J., Nwulu, N., & Bokoro, P. N. 2022. Optimal Placement and Operation of FACTS Technologies in a Cyber-Physical Power System: Critical Review and Future Outlook. In *Sustainability (Switzerland)* (Vol. 14, Issue 13). https://doi.org/10.3390/su14137707

Oleka, E. U., Ndubisi, S. N., & Ijemaru, G. K. 2016. Electric Power Transmission Enhancement: A Case of Nigerian Electric Power Grid. *American Journal of Electrical and Electronic Engineering*, *4*(1).

Ozcanli, A. K., Yaprakdal, F., & Baysal, M. 2020. Deep learning methods and applications for electrical power systems: A comprehensive review. In *International Journal of Energy Research* (Vol. 44, Issue 9). https://doi.org/10.1002/er.5331

Pardo-Zamora, O. N., Romero-Troncoso, R. de J., Millan-Almaraz, J. R., Morinigo-Sotelo, D., Osornio-Rios, R. A., & Antonino-Daviu, J. A. 2021. Power quality disturbance tracking based on a proprietary fpga sensor with gps synchronization. *Sensors*, *21*(11). https://doi.org/10.3390/s21113910

Penha da Silva Júnior, G., Figueiredo do Nascimento, T., & Sales Barros, L. 2021. *Comparison of Virtual Synchronous Generator Strategies for Control of Distributed Energy Sources and Power System Stability Improvement*. https://doi.org/10.48011/sbse.v1i1.2482

Polster, S., & Renner, H. 2017. Voltage stability monitoring methods for distribution grids using the Thevenin impedance. *CIRED - Open Access Proceedings Journal*, *2017*(1). https://doi.org/10.1049/oap-cired.2017.0297

Rahman, A. U., Syed, I., & Ullah, M. 2019. Small-signal stability criteria in AC distribution systems-a review. *Electronics (Switzerland)*, *8*(2). https://doi.org/10.3390/electronics8020216

Ramirez, L., & Dobson, I. 2014. Monitoring voltage collapse margin by measuring the area voltage across several transmission lines with synchrophasors. *IEEE Power and Energy Society General Meeting*, *2014-October*(October). https://doi.org/10.1109/PESGM.2014.6938974

Ramírez-P, S. L., Lozano-M, C. A., & Caicedo-D, N. G. 2018. Review and classification of indices for voltage stability monitoring using PMU measurements. In *Journal of Engineering Science and Technology Review* (Vol. 11, Issue 4). https://doi.org/10.25103/jestr.114.23

Ranjan Pradhan, S., Pragatika Bhuyan, P., Sahoo, S. K., & Satya Prasad, G. R. K. D. 2013. Design of Standalone Hybrid Biomass & PV System of an Off-Grid House in a Remote Area. *Journal of Engineering Research and Application Www.Ijera.Com*, *3*(6).

Rodriguez-Garcia, L., Perez-Londono, S., & Mora-Florez, J. 2019. An optimization-based approach for load modelling dependent voltage stability analysis. *Electric Power Systems Research*, *177*. https://doi.org/10.1016/j.epsr.2019.105960

Shair, J., Li, H., Hu, J., & Xie, X. 2021. Power system stability issues, classifications and research prospects in the context of high-penetration of renewables and power electronics. In *Renewable and Sustainable Energy Reviews* (Vol. 145). https://doi.org/10.1016/j.rser.2021.111111

Sharma, N., Acharya, A., Jacob, I., Yamujala, S., Gupta, V., & Bhakar, R. 2021. Major Blackouts of the Decade: Underlying Causes, Recommendations and Arising Challenges. *ICPS 2021 - 9th IEEE International Conference on Power Systems: Developments towards Inclusive Growth for Sustainable and Resilient Grid*. https://doi.org/10.1109/ICPS52420.2021.9670166

Tang, J., Zou, Z., Yang, J., Buticchi, G., & Hua, W. 2024. Adaptive Stabilizing Control of Smart Transformer Based on Reinforcement Learning Optimization. *IEEE Transactions on Industry Applications*, *60*(3). https://doi.org/10.1109/TIA.2024.3363108

Trias, A. 2018. HELM: The Holomorphic Embedding Load-Flow Method. Foundations and Implementations. *Foundations and Trends in Electric Energy Systems*, *3*(3–4). https://doi.org/10.1561/3100000015

Valuva, C., Chinnamuthu, S., Khurshaid, T., & Kim, K. C. 2023. A Comprehensive Review on the Modelling and Significance of Stability Indices in Power System Instability Problems. In *Energies* (Vol. 16, Issue 18). https://doi.org/10.3390/en16186718

Villa-Acevedo, W. M., López-Lezama, J. M., Colomé, D. G., & Cepeda, J. 2022. Long-term voltage stability monitoring of power system areas using a kernel extreme learning machine approach. *Alexandria Engineering Journal*, *61*(2). https://doi.org/10.1016/j.aej.2021.06.013

Yekini, S. M., Guiawa, M., Onyegbadue, I. A., & Olowoniyi, F. 2024a. Assessment of Sustainable Energy for Agricultural Energy Provision in Rural Sub-Saharan Africa. *African Journal of Agricultural Science and Food Research*, *15*(1), 61–76. https://doi.org/10.62154/sz7j2452

Yekini, S. M., Guiawa, M., Onyegbadue, I. A., & Olowoniyi, F. 2024b. Techno-Economic Optimization of Clean Energy Hybrid Systems in the Context of Assorted Battery Storage Technologies. *African Journal of Environmental Sciences and Renewable Energy*, *15*(1), 170–169. https://doi.org/10.62154/bh6yv490

Zhang, X., Hill, D. J., & Song, Y. 2023. A Load Dynamic Stability Index for Short-Term Voltage Stability Assessment and Control. *IEEE Transactions on Power Systems*, *38*(4). https://doi.org/10.1109/TPWRS.2022.3201942

Zhu, Y., Qi, B., & Milanović, J. V. 2016. Probabilistic ranking of power system loads for voltage stability studies in networks with renewable generation. *IEEE PES Innovative Smart Grid Technologies Conference Europe*. https://doi.org/10.1109/ISGTEurope.2016.7856274